PCCP

Accepted Manuscript

This is an *Accepted Manuscript*, which has been through the Royal Society of Chemistry peer review process and has been accepted for publication.

Accepted Manuscripts are published online shortly after acceptance, before technical editing, formatting and proof reading. Using this free service, authors can make their results available to the community, in citable form, before we publish the edited article. We will replace this *Accepted Manuscript* with the edited and formatted *Advance Article* as soon as it is available.

You can find more information about *Accepted Manuscripts* in the Information for Authors.

Please note that technical editing may introduce minor changes to the text and/or graphics, which may alter content. The journal's standard Terms & Conditions and the Ethical guidelines still apply. In no event shall the Royal Society of Chemistry be held responsible for any errors or omissions in this *Accepted Manuscript* or any consequences arising from the use of any information it contains.

ROYAL SOCIETY OF CHEMISTRY

www.rsc.org/pccp

Highly Efficient Functional $Ge_xPb_{1-x}Te$ based Thermoelectric Alloys

Yaniv Gelbstein and Joseph Davidow

Department of Materials Engineering, Ben-Gurion University of the Negev, Beer-Sheva 84105, Israel

Abstract.

Methods for enhancement of the direct thermal to electrical energy conversion efficiency, upon development of advanced thermoelectric materials, are constantly investigated mainly for an efficient implementation of thermoelectric devices in automotive vehicles, for utilizing the waste heat generated in such engines into useful electrical power and thereby reduction of the fuel consumption and CO_2 emission levels. It was recently shown that GeTe based compounds and specifically GeTe-PbTe rich alloys are efficient *p*-type thermoelectric compositions. In the current research, Bi_2Te_3 doping and PbTe alloying effects in $Ge_xPb_{1-x}Te$ alloys, subjected to phase separation reactions, were investigated for identifying the phase separation potential for enhancement the thermoelectric properties beyond a pure alloying effect. All of the investigated compositions exhibit maximal dimensionless figure of merit, *ZT*, values beyond 1 with the extraordinary value of 2.1, found for the 5% Bi_2Te_3 doped- $Ge_{0.87}Pb_{0.13}Te$ composition, considered as among the highest ever reported.

Introduction.

The dimensionless thermoelectric figure of merit, *ZT*, serving as an indicator to the efficiency of thermoelectric devices with respect to the involved materials is usually defined as $\alpha^2\sigma T/\kappa$, where, α- is Seebeck coefficient, *T*- the absolute temperature and σ, κ are the electrical and thermal conductivities, respectively. A representation of this figure in terms of the Fermi potential of the quantities appearing in *ZT*, using the classical statistics, is shown in eq. 1 [1].

$$ZT = \frac{\left(\frac{5}{2}+r-\eta\right)^2 T}{\left(2\frac{k^2}{e}FG\cdot\exp\eta\right)^{-1}+\left(\frac{5}{2}+r\right)T}, \quad F = \frac{\mu}{\kappa_l}\left(\frac{m^*}{m_0}\right)^{3/2}, \quad G = \left(\frac{2\pi m_0 kT}{h^2}\right)^{3/2} \qquad (1)$$

where, η- reduced Fermi energy (=E_F/kT), *r*- scattering parameter, *k* an *h*- Boltzmann and Plank constants, respectively, κ_l- lattice thermal conductivity, μ- the carriers mobility and *m**- the density-of-states effective mass.

From this expression, it is obvious that for *ZT* maximization, besides of optimal carrier concentration (strongly depends on η), the largest possible $F=\mu(m^*/m_0)^{3/2}/\kappa_l$ values are required. Many of the recently published mostly efficient thermoelectric materials are based on complicated semiconducting alloys (*e.g.* $Bi_2Te_{3-x}Se_x$ [2,3], $Bi_xSb_{2-x}Te_3$ [4-7], $PbTe_xSe_{1-x}$ [8], $Pb_xSr_{1-x}Te$ [9], $PbTe_xSe_{1-x}$ [10] and others), in which both κ_l and μ values are usually reduced compared to the pure constituents. The κ_l reduction is desirable for the enhancement of *ZT*, but the reduction of μ, is unwelcome. Due to these two opposite contributions to *ZT*, the thermoelectric enhancement for most of those previously published compositions was achieved by the generation of nano-features, serving as additional phonon scattering centers, leading to reduced κ_l values than those expected just by alloying. Due to the fact that for enhancement of *ZT*, t beyond the state of the art, both advanced methods for κ_l reduction (*e.g.* nano-structuring) and electronic optimization are required, the various factors influencing *ZT* for each investigated alloy should be understood in details.

In the current research, the thermoelectric potential of selected *p*-type GeTe-rich $Ge_xPb_{1-x}Bi_{2\delta}Te_{1+3\delta}$ (x=0.87, 0.82, 0.75, δ=3, 5%), compositions, correspond to 3 and 5 mol% Bi_2Te_3 doping levels of $Ge_xPb_{1-x}Te$, lying in the vicinity of the miscibility gap apparent in the quasi-binary PbTe-GeTe phase diagram (Fig. 1a), are investigated. Motivated by remarkable *ZT* >2, recently reported for the 3% Bi_2Te_3 doped - $Ge_{0.87}Pb_{0.13}Te$ composition [11], the influences of Bi_2Te_3 doping concentration, PbTe alloying level and the sub-micron involved structures on the thermoelectric potential of these alloys were studied and are discussed in details. For all of the investigated compositions, a major enhancement of the (μ/κ_l) factor, eq. 1, compared to the values expected just due to alloying effects (light blue colored bump above the theoretical blue dashed curve of Fig. 1a), attributing to

extremely high *ZT* values of up to 2.1 for the $Ge_{0.87}Pb_{0.13}TeBi_{0.1}Te_{1.15}$ composition (Fig. 1b), was associated with the presence of efficient phase separation sub-micron phonon scattering centers. Due to the fact that electronic properties' limitations, disable the extension of the maximal *ZT*, associated with any single composition, over a wide temperature range, practical possibilities of segmentation of these middle-temperatures $Ge_xPb_{1-x}Te$ thermoelectric alloys with the widely investigated $Bi_{0.5}Sb_{1.5}Te_3$ alloy, considered as one of the most efficient *p*-type compositions at lower temperatures of up to 350°C [7], Fig. 1b, are also discussed.

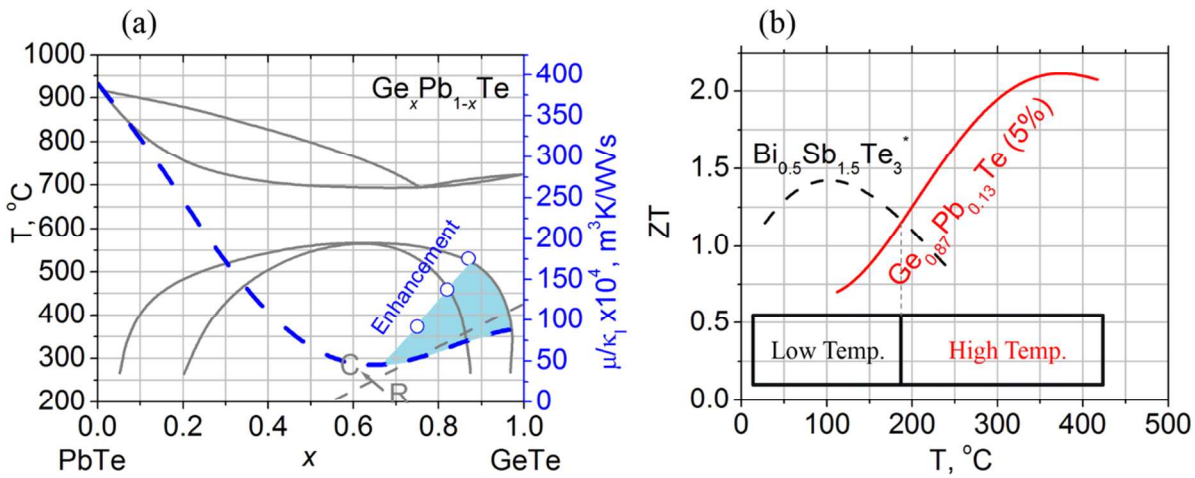

Fig. 1. (a) The quasi-binary PbTe-GeTe phase diagram (left axis) [12] and currently evaluated (μ/κ_l) factor variations (right axis) for the entire $Ge_xPb_{1-x}Te$ compositions range. The low temperature rhombohedral to cubic (R→C) phase transition is shown by the gray curve. (b) Temperature dependence of *ZT* of the currently developed $Ge_{0.87}Pb_{0.13}TeBi_{0.1}Te_{1.15}$ composition, (red curve) and the previously reported state of the art *p*-type $Bi_{0.5}Sb_{1.5}Te_3$ composition [7], highlighting the potential of segmentation for *ZT* enhancement over a wide temperature range.

Experimental.

Pure Ge, Pb, Bi and Te elements for obtaining *p*-type GeTe-rich $Ge_xPb_{1-x}Bi_{2\delta}Te_{1+3\delta}$ (x=0.87, 0.82, 0.75, δ=3, 5%) compositions were synthesized in a sealed evacuated (10^{-5} Torr) quartz ampoule by a rocking furnace at 1273K/1hour followed by water quenching. Hand crushed powder (60 mesh) using Agate mortar and pestle, was spark plasma sintered (SPS) (type HP D 5/1 FCT GmbH) at 823K/60min/25MPa.

The consolidated samples were found to be nearly fully dense (>96%). The samples crystal structure was analyzed by X-ray powder diffraction, XRD (Rigaku DMAX 2100 powder diffractometer). The microstructural characterizations and the chemical composition analysis were conducted by scanning electron microscopy (HRSEM; JEOL JSM-7400) and transmission electron microscopy (HRTEM; JEOL-2010).HRTEM, specimens were prepared by initially cutting disk-shaped tubes (Φ~3mm x ~5mm) from the spark plasma sintered sample using a custom designed electrode with an electron discharge machine, EDM. The samples were then sliced, again with the use of the EDM, into slices of ~200-300μm and hand polished with subsequently increasing grit (1000-1500) sand paper to about 70-100 μm in thickness. Subsequent thinning using Gatan precision dimple grinder and Gatan precision ion polishing system (PIPS) was applied for a final sample with a thin area transparent to electrons and a thickness of ~10-20nm. Seebeck coefficient and the electrical resistivity were measured by Linseis LSR-3/800 Seebeck coefficient / electrical resistance measuring system. The thermal conductivity, $\kappa=\alpha\rho C_P$ (α- thermal diffusivity, ρ- density C_P- specific heat) was determined by measurement of α and C_P individually by the flash diffusivity (LFA 457, Netzsch) and differential scanning calorimetry (STA 449, Netzsch) methods. The latter was also applied for determination of the phase transition temperature from the low temperature rhombohedral to the high temperature cubic phases. Lattice thermal conductivity, κ_l, was calculated by subtraction of the measured κ values from the electronic contribution to the thermal conductivity, $\kappa_e=L\rho^{-1}T$ (L- Lorentz number and ρ- measured electrical resistivity), in a procedure described previously [13], using the temperature and Fermi energy dependent Lorentz number, L, shown in eq. 2

$$L = \left(\frac{k}{e}\right)^2 \left[\frac{\left(r+\frac{7}{2}\right)\left(r+\frac{3}{2}\right)F_{r+5/2}(\eta)F_{r+1/2}(\eta)-\left(r+\frac{5}{2}\right)^2 F^2_{r+3/2}(\eta)}{\left(r+\frac{3}{2}\right)^2 F^2_{r+1/2}(\eta)}\right] \qquad (2)$$

where, $F_r(\eta)$ is Fermi integral .For evaluation of the room temperature carrier concentration and the electron mobility, Hall effect experiments were performed in a home-made apparatus using an electro-magnet of 1T and electrical currents in the range of 100-200mA, under a vacuum of 10^{-5} Torr. The Hall experimental setup, based on the configuration reported on [14]. For all of the transport properties measurements, the measurement errors are in the range of ±5%.

Results and Discussion.

Structural properties

All of the investigated GeTe- rich $Ge_xPb_{1-x}Bi_{2\delta}Te_{1+3\delta}$ compositions exhibit a room temperature characteristic XRD peaks doublet at 40.5 to 45.3^o, typical to the low temperature rhombohedral (*R3m*) phase of the predominant GeTe matrix, Fig. 2a. In this figure, although the δ=0.05 doping level, is referred as a representative case, a similar trend of peaks shift to higher (2θ) values with increasing of the GeTe concentration, *x*, is apparent also for δ=0.03, resulting from the smaller lattice parameter and planar spacing distance, d_{hkl}, of GeTe compared to PbTe (as can be seen from Bragg's law, $n\lambda=2d_{hkl}\sin\theta$). Since GeTe based alloys follow a second order phase transition from the low temperature rhombohedral to a high temperature *NaCl* cubic structure, at a compositional dependent temperature T_c (equals to 427°C for pure GeTe [15]), the specific T_c values of the various investigated compositions were identified by DSC, as shown in Fig. 2b.

In this figure, for each of the investigated Bi_2Te_3 doping concentrations, a reduction trend of the phase transition temperature with decreasing of the GeTe

concentration, x, (or increasing of the PbTe relative amount), was observed. Furthermore, for any given x composition, the phase transition temperature was decreased with increasing of the Bi_2Te_3 doping concentration. Both of these trends were expected since both Bi_2Te_3 and PbTe are uni-phase up to the melting temperature, and approaching to their pure compound's form, on account of the phase changed GeTe main component, is expected to decrease the phase transition temperature compared to 427°C of pure GeTe. From practical considerations, a second order phase transition at an intermediate temperature between the device's cold and hot side temperatures is preferable over first order transitions due to a continuous transformation from one structure to the other, inducing less thermal stresses on the thermoelectric leg under working conditions. Such misfit stresses, might be completely eliminated by segmentation of our investigated $Ge_xPb_{1-x}Te$ compositions with the lower temperature more efficient $Bi_xSb_{2-x}Te_3$ alloys (see Fig. 1b for example). However, such approach requires the reduction of the T_c values of the investigated $Ge_xPb_{1-x}Te$ alloys below 350°C, the maximal operation temperature of $Bi_xSb_{2-x}Te_3$. It can be seen from Fig. 2b that all of the $Ge_xPb_{1-x}Bi_{0.1}Te_{1.15}$ alloys and the $Ge_{0.75}Pb_{0.25}Bi_{0.06}Te_{1.09}$ composition fulfill this criterion.

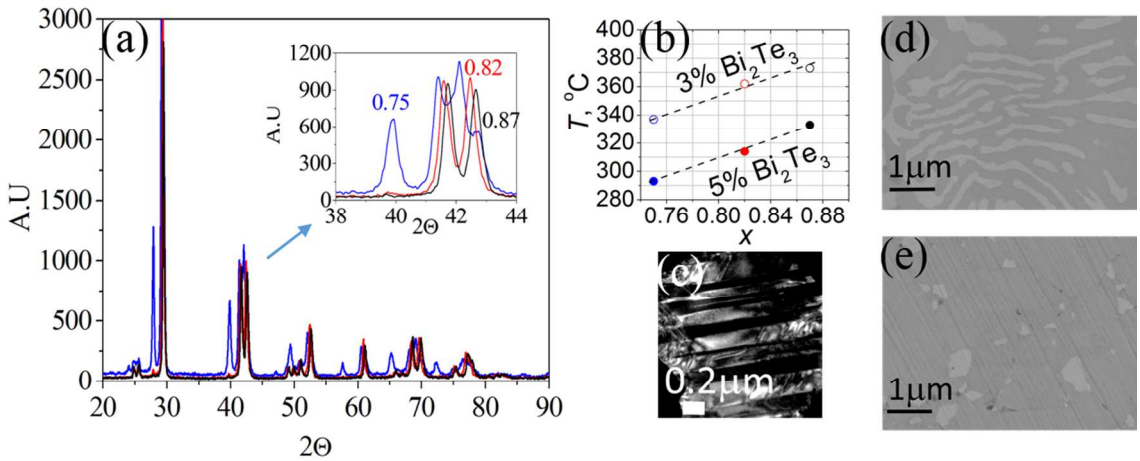

Fig. 2. (a) XRD analysis of the $Ge_xPb_{1-x}Bi_{0.1}Te_{1.15}$ alloys with an insert highlighting the doublet between 40°-45°. The 40, 41 and 43° peaks represent reflections from the (220), (104) and (110) planes repectively. (b) Second order

phase transtion temperatures of the different compostions, as were obtained by DSC. (c) TEM imaging of twins formed in $Ge_{0.87}Pb_{0.13}Bi_{0.06}Te_{1.09}$. HRSEM/BSE images of $Ge_xPb_{1-x}Bi_{0.1}Te_{1.15}$ alloys with x values of 0.75 (d) and 0.82 (e).

Typical microstructures of the investigated compositions are shown in Fig. $2_{c\text{-}e}$. Independent on δ, typical SEM micrographs of the investigated $Ge_{0.75}Pb_{0.25}Bi_{2\delta}Te_{1+3\delta}$ composition following SPS, clearly indicated a phase separation into PbTe rich- (bright lamellae) and GeTe rich- (dark matrix) phases in an disordered lamellar form (Fig. 2d), typical to spinodal decomposition, the dominant phase separation mechanism in the vicinity of this composition (the middle zone of the miscibility gap, Fig. 1a). For the case of the GeTe richer-$Ge_{0.82,0.87}Pb_{0.18,0.13}Bi_{2\delta}Te_{1+3\delta}$ alloys (x=0.82, 0.87), due to the dominating nucleation and growth, phase separation mechanism, in the vicinity of these compositions (the side areas of the miscibility gap, Fig. 1a), a typical microstructure containing bright nearly spherical PbTe rich- domains embedded in a darker GeTe rich matrix is clearly visible (Fig 2e). In both of these cases, the smaller dimensions of the phase separation domains are in the sub-micron range, expected to result in enhanced phonon scattering compared to the expected just by alloying of GeTe by PbTe. Higher magnification of the GeTe rich matrix revealed a dense population of sub-micron twins, as was observed by TEM, Fig. 2c, which might even enhance the phonon scattering effects and thereby reduce the lattice thermal conductivity even more.

Transport properties

The temperature dependent transport properties, Seebeck coefficient, α, electrical resistivity, ρ, thermal conductivity, κ, and the dimensionless figure of merit, *ZT*, for all of the investigated $Ge_xPb_{1-x}Bi_{2\delta}Te_{1+3\delta}$alloys are shown in Fig. 3.

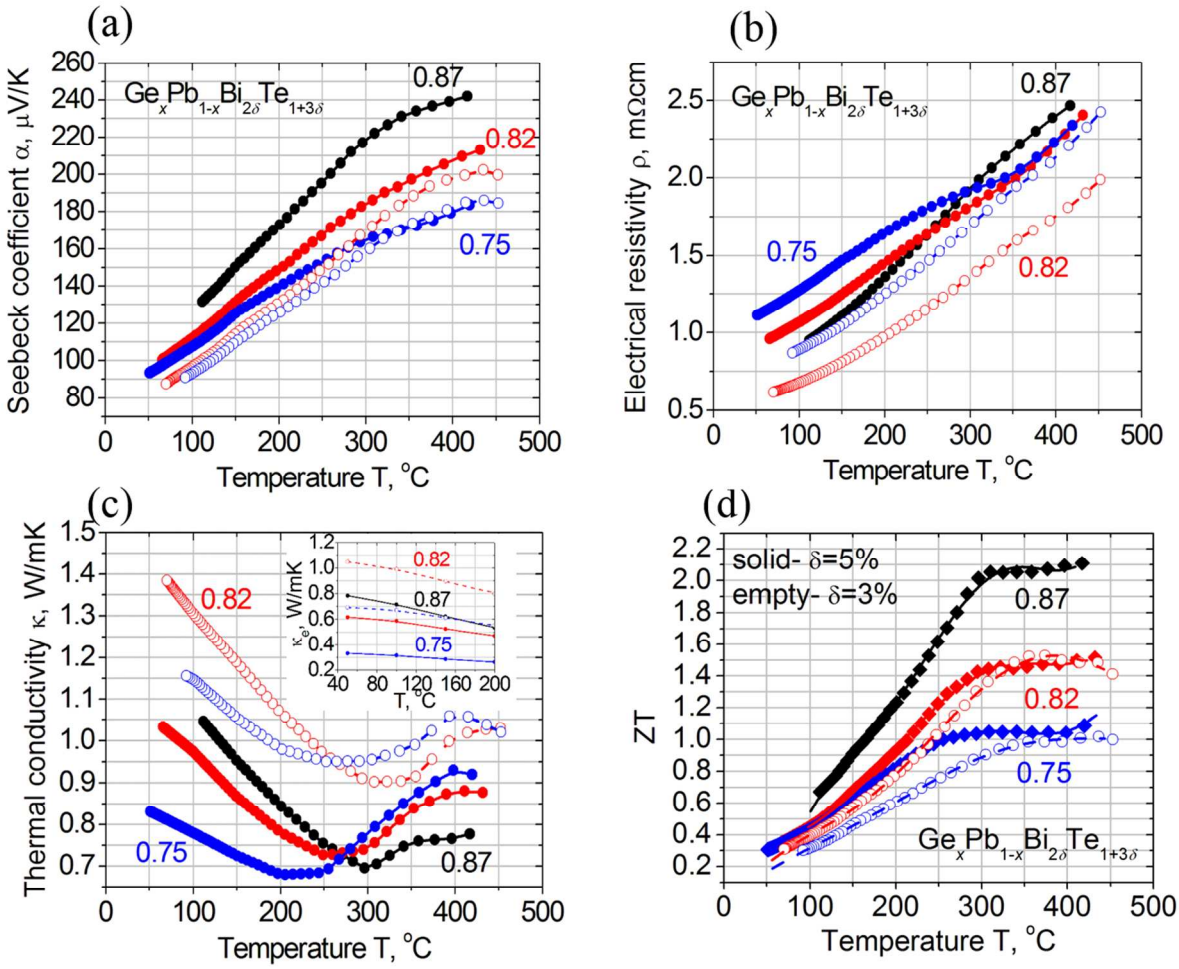

Fig. 3. Temperature dependence of Seebeck coefficient (a), electrical resistivity (b), thermal conductivity (c) and the dimensionless figure of merit, *ZT* (d) for all of the investigated $Ge_xPb_{1-x}Bi_{2\delta}Te_{1+3\delta}$alloys. The solid and dashed curves, as well as the solid and empty symbols, represent δ values of 5 and 3%, respectively.

From this figure it is clearly visible that for any given *x* value for the investigated $Ge_xPb_{1-x}Bi_{2\delta}Te_{1+3\delta}$alloys, increasing the δ value results in increased low temperature (below the phase transition temperature of each composition, Fig. 2b) α (Fig. 3a) and ρ (Fig. 3b) values and decreased electronic thermal conductivity, κ_e (the insert of Fig. 3c) values, indicating an expected donor doping action of Bi_2Te_3, resulting in decreased total carrier concentration, in agreement with the room temperature Hall effect experimental results, shown in Table 1. Such a donor effect is beneficial in GeTe rich alloys, which are usually *p*-type semiconductors containing very high holes concentrations (~$7x10^{26}m^{-3}$ for pure GeTe [16]), much

beyond the required optimal for thermoelectric applications. As can be seen from the table, the correspondent carrier concentrations of the investigated compositions are in the range of ~1.1×10^{26} and ~9.3×10^{25} m^{-3} upon δ values of 3% and 5%, respectively, which are much reduced toward optimal values compared to those of a pure GeTe compound.

The fact that for both of the investigated δ values, the low temperatures α values are nearly independent on the GeTe relative amount, *x*, while ρ and κ_e values increase and decrease, respectively, with the reduction of *x*, can be attributed to the decreased carrier mobility values with decreasing of the GeTe amount in the alloys, in agreement with the experimental Hall effect values, shown in Table 1.

Table 1. Carrier mobility and concentration, for the investigated compositions, as was determined from Hall effect measurements.

Composition	Mobility, cm^2/Vs	Carrier concentration , m^{-3}
$Ge_{0.87}Pb_{0.13}Bi_{0.1}Te_{1.15}$	73.83±3.69	$9.35\pm0.47\times10^{25}$
$Ge_{0.82}Pb_{0.18}Bi_{0.1}Te_{1.15}$	60.63±3.03	$9.33\pm0.46\times10^{25}$
$Ge_{0.75}Pb_{0.25}Bi_{0.1}Te_{1.15}$	45.82±2.29	$9.27\pm0.46\times10^{25}$
$Ge_{0.82}Pb_{0.18}Bi_{0.06}Te_{1.09}$	96.10±4.81	$1.15\pm0.06\times10^{26}$
$Ge_{0.75}Pb_{0.25}Bi_{0.06}Te_{1.09}$	65.87±3.29	$1.12\pm0.05\times10^{26}$

It is known that in solid solutions an additional carriers scattering mechanism is introduced due to the random distribution of different atoms in the same lattice site, an effect which was recently referred by Snyder et al. [17] as "*alloy scattering*". Thus, the mobility of a solid solution is lower than that of the pure predominant compound. In order to quantify this mobility reduction effect in $Ge_xPb_{1-x}Te$ alloys, the mobility, μ, dependence on the average carriers relaxation

time,τ, taking into account the various scattering mechanisms involved, τ_i, should be considered (eq. 3).

$$\mu = \frac{e\cdot\tau}{m^*}, \quad \tau^{-1} = \sum_i \tau_i^{-1} \qquad (3)$$

where, m^* is the effective mass.

τ's energy dependence is usually described in the form of $\tau = a\cdot E^b$, where a and b are two materials scattering constants and E is the carriers energy. In pure GeTe and PbTe compounds, the relaxation time is mainly contributed by the lattice vibration, $\tau_l = a_l\cdot E^{-1/2}$ [18], where a_l is the lattice scattering constant of the individual compound. As was described briefly above, upon the introduction of foreign atoms during alloying, in addition to lattice scattering, electron scattering is caused by the accompanied statistical potential aperiodicity. In pure compounds, for scattering by ionized impurity atoms, the relaxation time, τ_I, can be usually described as $\tau_I = a_I\cdot E^{3/2}$ [18], where a_I is the ionized impurity scattering constant. For the case of alloys, since it is known that the electrical resistivity, $\rho = \sigma^{-1} = (ne\mu)^{-1}$, where- σ-the electrical conductivity and n-carrier concentration, is proportional to relative amount of the alloying constituent (Matthiessen's rule), the relaxation time due to impurity scattering of alloys, $\tau_{I,Alloy}$, can be described in terms of eq. 4.

$$\tau_{I,Alloy} = \frac{a_{I,Alloy}\cdot E^{3/2}}{x(1-x)} \qquad (4)$$

where, $a_{I,Alloy}$ is the ionized impurity scattering constant due to the introduction of an alloying constituent, in a relative amount x.

Combining the two involved scattering mechanisms in $Ge_xPb_{1-x}Te$ alloys, in term of eq. 3, is described in eq. 5.

$$\frac{1}{\tau}=\frac{1}{\tau_l}+\frac{1}{\tau_{I,Alloy}}=\frac{E^{1/2}}{a_l}+\frac{x(1-x)}{a_{I,Alloy}\cdot E^{3/2}}\xrightarrow{yields}\tau=\frac{a_l\cdot a_{I,Alloy}\cdot E^{3/2}}{a_{I,Alloy}\cdot E^2+a_l\cdot x(1-x)} \qquad (5)$$

It can be seen from eq. 5, that for the specific case of pure compounds, x=0, τ is reduced to the $a_l\cdot E^{-1/2}$ expression, applies for the lattice scattering mechanism of the pure PbTe and GeTe compounds.

In general degeneracy, the carrier concentration, n, can be described in terms of eq. 6 [13].

$$n=\frac{4}{\sqrt{\pi}}\left(\frac{2\pi m^* kT}{h^2}\right)^{3/2}F_{1/2}(\eta) \qquad (6)$$

where, k and h are Boltzmann and Planck constants, respectively, T- the absolute temperature and $F_{1/2}(\eta)=\int_0^\infty \xi^{1/2}f_0(\eta)\,\partial\xi$ is Fermi integral. In this expression, $f_0=[1+\exp(\xi-\eta)]^{-1}$, is the Fermi distribution function and ξ, η are the reduced kinetic, $E/(kT)$, and Fermi, $E_F/(kT)$, energies, respectively.

Taking into account the energy dependence of n, eq. 6 and the τ expression applied for $Ge_xPb_{1-x}Te$ alloys, eq. 5, μ values can be determined from the expression, $\sigma=ne\mu$, following derivation of a σ(τ) dependence. In the general form, the electrical conductivity can be expressed as $\sigma=-\frac{e^2}{m^*}\int_0^\infty\frac{2E}{3}\frac{\tau\partial P}{\partial E}g(E)\,dE$ [17], where $g(E)dE = 4\pi(2m^*/h^2)^{3/2}E^{1/2}dE$ is known as the density of states and $P(E)=[e^{(E-EF)/kT}+1]^{-1}$ is the probability of occupation of a state of energy E. Substitution of τ, eq. 5, into this expression, leads to eq. 7.

$$\sigma_{Alloy}=-\frac{2}{3}\frac{4}{\sqrt{\pi}}\frac{e^2}{m^*}\left(\frac{2\pi\cdot m^*}{h^2}\right)^{3/2}\int_0^\infty\frac{a_l.a_{I,Alloy}.E^3}{a_{I,Alloy}.E^2+a_l.x(1-x)}\frac{\partial P}{\partial E}dE \qquad (7)$$

Finally, the mobility can be expressed in terms of eqs. 6-7, as shown in eq. 8.

$$\mu_{Alloy} = \frac{\sigma_{Alloy}}{n \cdot e} \quad (8)$$

The calculated room temperature mobility values, using eqs. 6-8 for the entire composition range of $Ge_xPb_{1-x}Te$ alloys are shown by the solid curve in Fig. 4a.

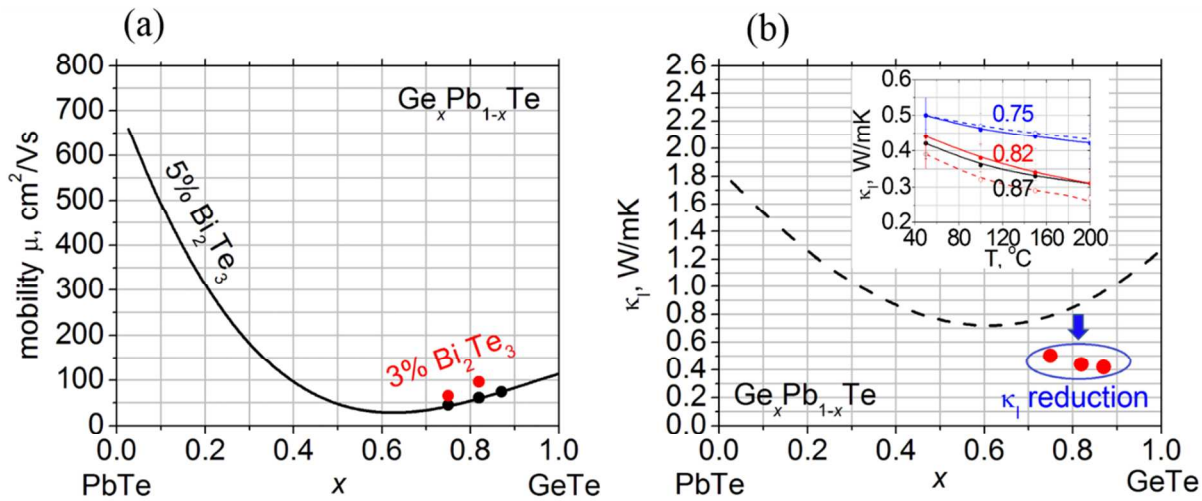

Fig. 4. (a) Room temperature experimental and calculated and measured mobility (a) and lattice thermal conductivity (b) values in the quasi binary GeTe-PbTe system.

In this calculation, a_l values for pure GeTe and PbTe compounds were obtained from the expression $a_l = \frac{\mu \cdot m^*}{e \cdot E^{-1/2}}$, based on equations 1 and 3 (using x=0), taking into account average carriers energy of $2kT$ below the top of the valence band, as typical for lattice scattering, and holes density-of state effective masses of $0.29m_o$ and $1.15m_o$ and holes mobility values of 1000 and 100 cm^2/Vs [19], for PbTe and GeTe, respectively. $a_{I,Alloy}$ values were obtained by fitting the calculated results to the measured values, shown in table 1. From this figure, the expected reduction trend of the mobility values just by alloying with increasing the PbTe concentration from 13% (x=0.87) via 18% (x=0.82) to 25% (x=0.75), as was noticed by the measured transport values and explained in details related to Fig. 3 and Table 1. The slight mobility reduction observed by the experimental values

upon increasing the δ value for each of the investigated alloys, can be attributed to an increased lattice disordering, compared to the expected just by GeTe-PbTe alloying. It is noteworthy that the above mobility calculations, taking into account nominal *x* values in $Ge_xPb_{1-x}Te$ alloys, assume samples uniformity. Due to the fact that in the investigated alloys, a coherency is maintained between the alternating phase separated GeTe and PbTe rich domains, an additional significant mobility reduction due to the phase separation reaction is not expected.

The current analysis is useful for estimation of the general mobility reduction trends upon PbTe alloying of GeTe, compared to the associated values of the pure compounds but only accurate for solution treated alloys (beyond the miscibility gap).

The lattice thermal conductivity values, obtained by subtraction of the electronic from the measured thermal conductivity values (Fig. 3c) are shown in Fig. 4b. This figure also clearly shows a major reduction of the obtained κ_l values than the expected ones just due to alloying, as visible by comparing the measured room temperature values to the dashed "*alloying*" curve published recently [20]. This up to 50% reduction, which can be explained in terms of the enhanced phonon scattering by the phase separation features described previously related to Fig. 2, is attributing to the enhanced (μ/κ_l) values described in the introduction paragraph related to Fig. 1a and to the high measured *ZT* values (Fig. 3d). As can be seen by Fig. 3d, very high *ZT* values were observed for the investigated alloys with an extraordinary maximal value of ~2.1 found for the $Ge_{0.87}Pb_{0.13}Bi_{0.1}Te_{1.15}$ composition. Moreover, this specific highly efficient composition, can be easily segmented to the efficient low temperature $Bi_xSb_{2-x}Te_3$ alloys, due to a lower phase transition temperature (~330°C, Fig. 2b) than the maximal operation temperature of

the latter (350°C), resulting in higher average *ZT*s over the large temperature gradients frequently required in practical applications.

Conclusions.

In the current research, *p*-type $Ge_xPb_{1-x}Bi_{2\delta}Te_{1+3\delta}$ alloys with *x* values in the vicinity of the miscibility gap of the quasy-binary GeTe-PbTe phase diagram were investigated for obtaining highly efficient thermoelectric materials for the temperatures range of up to 450°C. All of the investigated compositions exhibit a phase transition from low temperature rhombohedral to high temperature cubic phases at decreased temperatures with increasing of the doping (δ values) and PbTe relative amounts. All of the investigated alloys exhibit maximal *ZT* values higher than 1 with an extraordinary maximal value of ~2.1 found for the $Ge_{0.87}Pb_{0.13}Bi_{0.1}Te_{1.15}$composition, associated with the presence of sub-micron phase separation features attributing to increased μ/κ_l values beyond the expected values just by alloying of PbTe into GeTe. Furthermore, the reduced phase transition temperatures for most of the investigated compositions, including the mostly efficient $Ge_{0.87}Pb_{0.13}Bi_{0.1}Te_{1.15}$ composition, below the maximal operating 350°C temperature of the lower temperatures *p*-type $Bi_xSb_{2-x}Te_3$ state of the art alloys, exhibit a high potential for obtaining higher average *ZT*s than all of the *p*-type compositions ever reported for the temperatures range of 50-450°C, upon segmentation of these two material classes.

Acknowledgement.

The work was supported by the Israel Science Foundation (ISF), Grant Nos. 497/12 and 1578/12.

References.

1. H.J. Goldsmid, Applications on thermoelectricity, edited by B.L. Worsnop, John Wiley and Sons 41 (1960).
2. N. Gothard, X. Ji, J. He and Terry M. Tritt, Thermoelectric and transport properties of *n*-type Bi_2Te_3 nanocomposites, *Journal of Applied Physics* **103** 054314 (2008).
3. Wei-Shu Liu, Qinyong Zhang, Yucheng Lan, Shuo Chen, Xiao Yan, Qian Zhang, Hui Wang, Dezhi Wang, Gang Chen and Zhifeng Ren, Thermoelectric Property Studies on Cu-Doped *n*-type $Cu_xBi_2Te_{2.7}Se_{0.3}$ Nanocomposites, *Adv. Energy Mater.* **1** 577–587 (2011).
4. Yi Ma, Qing Hao, Bed Poudel, Yucheng Lan, Bo Yu, Dezhi Wang, Gang Chen and Zhifeng Ren, Enhanced Thermoelectric Figure-of-Merit in p-Type Nanostructured Bismuth Antimony Tellurium Alloys Made from Elemental Chunks *Nano Lett.,* **8**(8) 2580-2584 (2008).
5. Wenjie Xie, Xinfeng Tang, Yonggao Yan, Qingjie Zhang, and Terry M. Tritt, Unique nanostructures and enhanced thermoelectric performance of melt-spun BiSbTe alloys, *Applied Physics Letters* **94**, 102111 (2009).
6. O. Ben-Yehuda, Y. Gelbstein, Z. Dashevsky, R. Shuker and M.P. Dariel, Highly textured Bi_2Te_3-based materials for thermoelectric energy conversion, *Journal of Applied Physics* **101**, 113707 (2007).
7. Bed Poudel, Qing Hao, Yi Ma, Yucheng Lan, Austin Minnich, Bo Yu, Xiao Yan, Dezhi Wang, Andrew Muto, Daryoosh Vashaee, Xiaoyuan Chen, Junming Liu, Mildred S. Dresselhaus, Gang Chen, Zhifeng Ren**,** High-Thermoelectric Performance of Nanostructured Bismuth Antimony Telluride Bulk Alloys, *Science* **320** 634-638 (2008).
8. Yanzhong Pei, Xiaoya Shi, Aaron LaLonde, Heng Wang, Lidong Chen & G. Jeffrey Snyder, Convergence of electronic bands for high performance bulk thermoelectrics, *Nature* **473** 66-69 (2011).
9. Kanishka Biswas, Jiaqing He, Ivan D. Blum, Chun-I Wu, Timothy P. Hogan, David N. Seidman, Vinayak P. Dravid and Mercouri G. Kanatzidis, High Performance Bulk Thermoelectrics with All Scale Hierarchial Architectures, *Nature* **489** 414-418 (2012).
10. John Androulakis, Chia-Her Lin, Hun-Jin Kong, Ctirad Uher, Chun-I Wu,Timothy Hogan, Bruce A. Cook, Thierry Caillat, Konstantinos M. Paraskevopoulos and Mercouri G. Kanatzidis, Spinodal Decomposition and Nucleation and Growth as a Means to Bulk Nanostructured Thermoelectrics: Enhanced Performance in $Pb_{1-x}Sn_xTe$-PbS, *J. Am. Chem. Soc.* **129** 9780-9788 (2007).
11. Yaniv Gelbstein, Joseph Davidow, Steven N. Girard, Duck Young Chumg and Mercouri Kanatzidis, Controlling metallurgical phase separation reactions of the $Ge_{0.87}Pb_{0.13}Te$ alloy for high temperature performance, *Advanced Energy Materials* **3** 815-820 (2013).
12. S. Gorsse, P. Bauer Pereira, R. Decourt and E. Sellier, Microstructure engineering design for thermoelectric materials: an approach to minimize thermal diffusivity, *Chem. Mater.* **22** 988-993 (2010).
13. Y. Gelbstein, Z. Dashevsky and M.P. Dariel, High performance *n*-type PbTe-based materials for thermoelectric applications, *Physica B* **363** 196-205 (2005).
14. O. Appel and Y. Gelbstein, A comparison between the effects of Sb and Bi doping on the thermoelectric properties of the $Ti_{0.3}Zr_{0.35}Hf_{0.35}NiSn$ half-Heusler alloy, *Journal of Electronic Materials* **43**(6) 1976-1982 (2014).
15. Joesph Davidow and Yaniv Gelbstein, A comparison between the mechanical and thermoelectric properties of three highly efficient *p*-type GeTe-rich compositions: TAGS-80, TAGS-85 and 3% Bi_2Te_3-doped $Ge_{0.87}Pb_{0.13}Te$, *Journal of Electronic Materials* **42**(7) 1542-1549 (2013).
16. Y.Gelbstein, O. Ben-Yehuda, E. Pinhas, T. Edrei, Y. Sadia, Z. Dashevsky and M.P. Dariel, Thermoelectric properties of (Pb,Sn,Ge)Te based alloys, *Journal of electronic materials*, **38**(7) 1478 (2009).
17. Heng Wang, Aaron D. LaLonde, Yanzhong Pei and G. Jeffrey Snyder, The criteria for beneficial disorder in thermoelectric solid solutions, *Adv. Funct. Mater.* **23** 1586-1596 (2013).
18. G.C. Jain and W.B. Berry, Transport properties of solids and solid state energy conversion, McGraw-Hill, pp. 25-27 (1972).
19. Yu. I. Ravich, B.A. Efimova and I.A. Smirnov, Semiconducting lead chalcogenides, Edited by L.S. Stil'bans, Plenum Press, New-York pp. 352-354 (1970).
20. Yaniv Gelbstein, Joseph Davidow, Ehud Leshem, Oren Pinshow and Strul Moisa, Significant Lattice Thermal Conductivity Reduction following Phase Separation of the Highly Efficient $Ge_xPb_{1-x}Te$ Thermoelectric Alloys, *Phys. Status Solidi B* 1-7 (2014)..